https://dx.doi.org/10.1016/j.apor.2019.04.012

A simple experimental method to regain the mechanical behavior of naturally structured marine clays

Usama Khalid
Department of Civil Engineering and State Key Laboratory of Ocean Engineering,
Shanghai Jiao Tong University, Shanghai, 200240, China
engr.usamakhalid@sjtu.edu.cn

Guan-lin Ye*
Department of Civil Engineering and State Key Laboratory of Ocean Engineering,
Shanghai Jiao Tong University, Shanghai, 200240, China
ygl@sjtu.edu.cn

Santosh Kumar Yadav
Department of Civil Engineering and State Key Laboratory of Ocean Engineering,
Shanghai Jiao Tong University, Shanghai, 200240, China
yadavsantoshkr@sjtu.edu.cn

Zhen-Yu Yin
Department of Civil and Environmental Engineering
The Hong Kong Polytechnic University, Hung Hom, Kowloon, Hong Kong
zhenyu.yin@polyu.edu.hk

*Corresponding Author
Guan-lin YE
Professor
Department of Civil Engineering
Shanghai Jiao Tong University
800# DongChuang RD, Minhang District, Shanghai, China. 200240
Email: ygl@sjtu.edu.cn

This manuscript was submitted to Applied Ocean Research, October 2018.

Abstract: Quantitative laboratory studies on the structural behavior of natural intact marine clays require a large number of identical natural samples leading to an expensive and challenging task. This study proposes a simple method to reconstruct an artificial structured marine clay as the state of its natural intact clay at both macro and micro levels. For this purpose, the Shanghai marine clay is selected and mixed with low cement contents (1-6%). The clay-cement slurry is mixed in a container with the ice-covered sides at a low temperature about 0±2 °C to postpone the hydration reactions until consolidation began. The purpose of adding cement is to generate the inter-particle bonding and structure in reconstituted samples. Initially, the reconstituted samples are consolidated under the in-situ stress of 98 kPa and then under the pre-consolidation pressure of 50 kPa. Mechanical characteristics such as compression index, yield stress, unconfined compression strength, shear strength ratio, and the stress paths from triaxial tests are compared with natural intact clay accordingly. Scanning electron microscope and mercury intrusion porosimetry analyses are also performed to analyze the microstructure of clays for comparison. Furthermore, the proposed method is also examined by using natural intact marine clays of different locations and characteristics.

Keywords: Structured marine clay; reconstruction method; stress path; compressibility; microstructure.

1. Introduction

The combined effects of fabrics, inter-particle forces and their composition are called soil structure, whereas, the term "fabric" is the arrangement of particles, particle groups and pore spaces [1]. Structured marine clays are originated in coastal, marine, deltaic or by the combination of depositional environment. Such deposition has been occurred during the past 20,000 years in the last phase of the Pleistocene period [2]. These clays have complex geotechnical behaviors due to a combination of various environmental, geologic and chemical processes during the deposition. These clays are habitually encountered and dealt in ocean geotechnical engineering [3,4], and constitute one of the typical strata in the shallow range of deep-water seabed [5,6]. Such clays are considered to be as the problematic soils because of high compressibility, poor shear strength and high-water content which cause a severe construction challenge for the geotechnical engineers in the marine environment [7-10]. Since the strength of such clays is generally governed by their structure [11] which becomes unstable and break down under loading, the soil structure assessment of such kinds of clays becomes crucial.

Soil structure is an inherent property of natural clays; since the soil structure is a combination of fabric and inter-aggregate bonding [12], it has a substantial effect on the mechanical characteristics of clays [13-15]. The structured marine clay deposits depend on their consolidation history, deposition, sedimentation, and subsequent straining [7,16,17], and usually, these features cannot be traced down, precisely, for most natural clays [18,19]. However, these deposits express the destructuration during straining due to the quick loss of inter-aggregates bonding [17], which complicates the sampling of natural intact clay. Since the natural samples are more or less disturbed with variations, it becomes difficult to get identical samples, and thus it makes quantitative relationship between the structure and the mechanical characteristics of natural clayey samples questionable. To seek an effective way, artificial generating of a structured clay could be a good choice. In such case, precise reconstruction of artificially structured clay samples close to the natural soils is a crucial consideration.

Limited literature is available on the reconstituted methods of soft clays that try to generate similar mechanical behavior to that of natural intact clays. Bjerrum and Rosenqvist [20] tried to reconstitute the Norwegian clay by deposition in salt water performing a lengthy procedure of twenty-three months. Pusch and Arnold [21] reconstituted the quick clay from the illite powder. The organic material from illite was removed using peroxide, later the illite was deposited in sea water with a salinity of 35 g·L^{-1}. The sensitivity was increased from 2.1 to merely 3.7 after consolidation and leaching in a geotechnical centrifuge, consequently not characterizing the quick clay. Kamon and Nagao [22] reconstituted the cemented clays using the sodium silicate by 5% in weight. These clays showed larger compressibility, yield stress and undrained strength than the non-cemented clays. Tsuchida et al. [23] duplicated the compression behavior of natural intact clays by consolidating the clay slurry at a high temperature. This is because the key advantage of high temperature consolidation is to increase the cementation action. Meijer and Dijkstra [24] reconstructed small sized (25 mm in Height) quick clay samples by leaching using the geotechnical centrifuge, resulting in low undrained strength and high void ratio compared to the natural intact sample. Udaka et al. [25] also reconstituted the samples using cement content and tried to duplicate the natural compression behavior of clays without equating it to the natural intact clays. Regardless of an inadequate success in the past, a method is still needed to reconstruct the artificially-structured clays. The first advantage of such approach is the freedom to reconstitute the samples of any shape and size for laboratory modeling. Secondly, it can also reduce the need for expensive natural intact sample having the soil structure disturbance. Thirdly, this method can also allow the reuse of obtained samples for quantitative studies regarding the soil structures and mechanical characteristics.

Because of the aforementioned reasons, a new, simple, inexpensive and time-efficient method is devised which can reconstitute the structured clay and replicate the geotechnical behaviors similar to the natural intact clay. The proposed method is close enough to the natural structuration process of structured marine clays. To generate the flocculation and cementation in soil structure, low cement content is used. The soil-cement slurry is consolidated under a certain pressure to avoid the time-consuming natural structuration process. Undrained triaxial tests, oedometer tests, and unconfined compression tests are performed on both artificially-structured and natural intact clay samples to examine their similarity at the macro level. The microstructures of natural intact and reconstituted clays are investigated by mercury intrusion porosimetry (MIP) and scanning electron microscope (SEM) analyses. Furthermore, different Shanghai marine clays are reconstituted with the analogous mechanical behavior of their natural intact samples.

2. Effect of cement on the structure of marine clays

Due to the addition of cement in clays, interparticle forces become negative due to the tensile resistance of cemented bond, which increases the strength of cemented clay [26]. Many researchers [27-33] have studied the mechanical characteristics and microstructure formation within the soil skeleton due to the cement under different curing times and reconstituted methods in the recent years. The use of cement as an additive to improve the stiffness and strength of marine clays is also well recognized [34-37]. Increasing cement content decreases the soil ductility, which has also been observed by various researchers as a large post peak fall in the strength of the cemented soil [27,32]. The yield stress of cemented clay is higher than the untreated one, and an increasing behavior of yield stress with cement leads to a sharp decrease in the void ratio. This trend is also perceived in natural structured soils [38,39], and the mechanical characteristics of both natural and reconstituted soils are governed by their structures [40].

Due to the addition of cement, the microstructure of clays affects by the formation of calcium ions in interlayer which enhances the attraction between clay particles and procedure the flocculated aggregates [28]. The cementation products such as calcium silicate hydrates (CSH), calcium aluminate hydrates (CAH) and calcium aluminum silicate hydrates (CASH) are formed in clay-water mixture with cement addition [41]. These cementation products improve the inter-aggregate bonding, reduce the pores, and increase the strength of clayey soils [27,30].

With increasing curing time, the cementitious products fill the large sized pores and increases the volume of small-sized pores [28,30,42].

3. Materials and methods

3.1 Shanghai marine clay

Shanghai is located in the Yangtze river delta in east China as shown in Fig. 1. The Yangtze river has deposited a large volume of fine sediments in the last 20,000 years. Up to 30 to 40m depth, these sediments have soft deltaic nature and are distributed into five layers of soft marine clays by their depositional history, mechanical and physical characteristics [43,44]. These clays are also recognized as Shanghai marine clays. Deposition of these clays has occurred due to the Pleistocene sediments (mainly silty clay) and Holocene sediments (silty clay, mucky silty clay) [44,45]. The engineering characteristics of Shanghai clays are affected by the depositional environment. Shanghai clay from the 4th layer of stratum was selected for this research because it has a significant effect on underground construction [46-50]. It is a traditional structured marine clay with high compressibility, low strength, and high-water content. Two structured marine clays were collected from two different sites for the development and validation of reconstituted method. Disturbed and natural intact samples were collected from an excavation site of Putuo District, Shanghai from the depth of 12m for method development. The natural intact samples were collected using the block sampling method. The block sides were sealed with wax and wrapped with polyethene shrink sheet to avoid sample disturbance and water evaporation [51]. The clay, silt and sand contents are 24%, 74%, and 2% respectively, in this sample, and the values of liquid (w_L) limit and plasticity index (I_p) are 36.6% and 16.94 % respectively. A sample for method validation was collected from a construction site of Minhang District, Shanghai from the depth of 16m. The clay, silt and sand contents in the sample are 40%, 59%, and 1% respectively, and values of liquid limit and plasticity index are 45.5% and

121.35% respectively. Both samples are classified as low plastic clay (CL) based on the Unified Soil Classification System. The physical and mechanical characteristics of both samples are presented in Table 1.

3.2 Reconstitution method of structured clay

Reconstitution method was divided into two parts; clay-cement slurry composition, and slurry consolidation under effective vertical pressure. To make the slurry, the oven-dried pulverized clay was passed from 2 mm sized sieve to remove the impurities, and the de-aired distilled water was mixed in subjected clay. The initial water content ratio of clay slurry was $1.5w_L$. When consolidation of soft clay deposits on seabed commences in natural conditions, the water content is considered to be 1.5 to $2w_L$ [25]. Before adding the cement, the slurry was passed through 0.5 mm sized sieve for further refinement, and mixed and cooled for approximately half an hour to keep the temperature about 0±2 °C. The motive of reducing slurry temperature was to postpone the chemical hydration reaction between clay and cement until consolidation instigated. Mitchell and Soga [26] explained that cementation erupts during or after applying the consolidation pressure in natural clays which produce additional forces between particles contents. Henceforth, the cementation conditions of natural clay were achieved by keeping the clay-cement slurry temperature low. For this, the slurry container sides were covered with ice-water mixer. The cement slurry was prepared at a water-cement ratio (*w/c*) of 1.0 for better workability and was mixed about 2 minutes to break the particles lumps. Subsequently, both slurries were mixed for 10 minutes and transferred into the consolidation tube. A fine ordinary Portland cement was used with different fractions for this study, and its physicochemical characteristics are given in Table 2. The consolidation tube with the size of 15 cm in diameter, and 35 cm in height was used for consolidation purpose as shown in Fig. 2. Slurries were consolidated under one-dimensional vertical pressure (Reconstituted pressure). To determine the effect of reconstituted pressure on the method, samples were consolidated under different reconstituted pressures of 98 kPa and 50 kPa. The pre-consolidation pressure of the undisturbed state was 50 kPa whereas the in-situ stress of the soil was 98 kPa. Based on these values, one set of samples was consolidated at the pre-consolidation pressure, and other was consolidated at the in-situ stress. The reconstituted pressures were applied step by step in 14 days to consolidate and drain the slurries. Because in natural conditions, the pressure increases with the time and the strength development due to cementation and the consolidation take place at the same time. After 14 days, the large-sized samples were obtained from molds and cut according to required sizes. To avoid the water evaporation from samples, the samples were stored in the desiccators after wrapping the polyethene shrink sheet for self-curing at 20±5 °C [51].

3.3 Determination of required percentage of cement content

A trial-based method is used to determine the minimum cement content (c_0) at which the clay structure is affected. This method is recommended by Tang et al. [50], and the required amount of cement is governed by the unconfined compression strength (q_u). The relationship between cement content (%) and unconfined compression strength (q_u) is given in Eq. (1):

$$q_u = k(c - c_0) \tag{1}$$

where, k is the strength coefficient (kPa/%), and c_0 is the minimum cement content required to increase the q_u with curing time, and its value is determined by a linear relationship between the cement content (c) and the unconfined compressive strength. For this study, the required percentage of cement for shanghai marine clay is determined from a relationship of q_u and cement content given in Eq. 1.

The relationship between cement content and the unconfined compressive strength of Shanghai marine clay is established in Fig. 3. Samples were reconstituted at 98 kPa vertical pressure and cured at 7, 14, and 21 days. The k-value increases with an increase in the curing time, and an average k-value for selected marine clay is 21.39 kPa/% and all trend lines in Fig. 3 have the same R^2-value (correlation coefficient) of 0.99. The c_0-value is 2% for clay taken because of the q_u-value increases with an increase in the curing time at 2% cement content. However, the increment in q_u-value of 1% cemented sample is insignificant compared to untreated sample and also remains unchanged with curing time. It is a trial-based method. Consequently, 1%, 2%, and 3% cement contents were selected for further study.

To determine the c_0-value for reconstituted clays, a lengthy procedure to perform a series of unconfined compression tests at different cement contents and curing times can be avoided by using the relationship of liquid limit and the c_0-values developed in Fig. 4. The liquid limit (w_L) and the c_0-value show a good dependency on each other. This relationship is drawn by using the data of six marine clays. Out of six, data of five Japanese marine clays are taken from previous research [25], and the Atterberg's limits and the c_0-values of these clays are presented in Table 3. The expression between the liquid limit and the c_0-value is proposed in Eq. 2.

$$c_0(\%) = 0.0012w_L^2 - 0.1059w_L + 4.144 \tag{2}$$

The R^2-value is 0.84. A good and reliable correlation must have a high value of R^2, and its value indicates a good accuracy to predict the c_0-values of other marine clays.

3.4 Test methods

Delage et al. [52] freeze-drying technique was used to prepare the MIP and SEM samples. The 125 mm^3 sized samples were cut with a scalpel to avoid soil structure disturbance. The specimens were frozen in isopentane which was cooled to its melting point in liquid nitrogen.

This process avoids gaseous bubbling caused by direct immersion of soil specimens in liquid nitrogen at -196 °C. During quick freezing, the temperature of the samples was -130 °C to avoid ice crystals formation. The vacuum freeze dryer was used for sublimation of water at -70 °C.

Scanning electron microscope (SEM) analyses were accomplished to visualize the microstructural deviations in the clay structure. The samples were positioned on the aluminum stubs and shielded the sides with conducting tape. The ion sputter (Hitachi E-1045) was used to deposit a thin metal coating of gold (Au) on the samples' surface which made them electrically conductive and also facilitated to avoid charge build-up during the observation. After this, the SEM analyses were performed using Field Emission Scanning Electron Microscope (Philips FEI Sirion 200) apparatus.

The pores sizes and their distributions in microstructures of reconstituted and natural intact samples were analyzed using AutoPoure IV 9500 (Micromeritics) mercury intrusion porosimeter (MIP). The MIP working is based on Washburm [53] principle.

$$p = -\frac{4\sigma_{Hg}\cos\theta}{d} \quad (3)$$

where, p is applied pressure of mercury intrusion (maximum 225 MPa in this study); θ is the mercury-soil contact angle (130° in this study); σ_{Hg} is the surface tension (485 dynes/cm at 25 °C); d is the pore diameter.

One-dimensional oedometer tests were performed to determine the compressibility behavior of samples. Oedometer rings of 2 cm in height, and 6 cm in diameter were used to cut the required sized samples from a sizeable sample. Consolidation pressures were applied from 12.5 to 1600 kPa in eight steps. Duration of each pressure was 24 hrs.

A computerized GDS triaxial apparatus [54] was used to conduct the consolidated undrained triaxial (CU) tests. The effective confining and back pressures were 10 and 100 kPa respectively, during the saturation stage. During the shear and consolidation stages, the effective confining pressure applied was 200 kPa. The samples were tested with the displacement rate of 0.011 mm/minute and this adopted strain rate facilitated to achieve a more uniform distribution of pore water pressure within the sample, particularly at the time of failure. The unconfined compressive tests were performed to determine the shear strength of the reconstituted and natural intact samples. The sample size was of 3.91 cm in diameter, and 8 cm in height. The tests were performed at the shearing rate of 1 mm/min. Table 4 shows the details of tests conducted for this study concerning different cement contents, reconstituted pressures and curing times.

4. Macrostructure results and discussion

4.1 Unconfined compressive strength

Unconfined compression tests were performed to determine the shear strength of the reconstituted and natural intact samples. Fig. 5a illustrates a comparison of stress-strain curves of reconstituted and the natural intact samples. The stress-strain behavior of cemented clay shows ductile, semi-brittle and brittle behavior at different cement contents. It is examined that with increasing cement content, the peak axial stress increases while corresponding strain decreases. Meanwhile, the increment in the formation of calcium silicate hydrates (CSH) with cement content causes an increase in the unconfined compression strength [55,56]. The q_u-value of the intact sample is almost the same as the value of 2% cemented sample. However, the stress-strain response of the intact sample curve is more ductile as compared to 2% cemented sample.

Shear strength ratio ($q_{u(Intact)}/q_{u(untreated)}$) of the natural intact sample is 2.44 as shown in Fig. 5b. The ranges of shear strength ratios ($q_{u(cemented)}/q_{u(untreated)}$) for 1%, 2%, and 3% cemented samples are 1.43-1.49, 2.4-3, and 3.95-4.21 at different curing time respectively. Hence, the shear strength ratio of the natural intact sample is almost the same as 2% cemented sample.

4.2 Compression characteristics

One-dimensional oedometer tests were performed to analyze the effect of cement content on macrostructure of clay concerning initial void ratio (e_0), compression index (C_c), swell index (C_s), and yield stress (σ_y).

4.2.1 Effect of cement content on the reconstituted method with respect to compression characteristics

Comparison of *e*-log(*P*) relationships for reconstituted and natural intact samples are presented in Fig. 6a. These samples were reconstituted at 98 kPa. The yield stresses (σ_y) of reconstituted samples and pre-consolidation pressure of natural intact samples were calculated by using the Casagrande method [57]. In this study, the pre- and post-yield regions are the parts of compression curve before and beyond the yield stress respectively. There is a minor change of the void ratio in the pre-yield region due to strong interparticle bonding while the applied consolidation pressure is also lower than the yield stress of reconstituted samples. However, in the post-yield region, the void ratio decreases promptly due to the breakage of cementation bonds (destructuration) [27].

Moreover, all bonds are not broken down when the yield is initiated, and only those bonds subjected to stresses are demolished [58]. The σ_y-values of reconstituted samples due to structure reflect the bond strength [11] and this bond strength is possibly due to cement content and reconstituted pressure [32]. Consequently, the yield stress of cemented soils increases with the increment of cement content and reconstituted pressure. Moreover, the initial void ratio increases with increasing the cement content because samples were reconstituted under pressure. Due to the reconstituted pressure, the void ratio decreases due to the dissipation of water and air. Meanwhile, the hydration reaction also starts, and cemented samples begin to harden up. Consequently, the sample having more cement content gain more structure (strength) in short time and the effect of pressure on void ratio decline and sustain more void ratio as compared to the sample treated with less cement.

Figure 6b describes the effect of cement content on compression index (C_c). The values of C_c are calculated at each consolidation pressure and the relationship between C_c and log(P) is drawn in logarithmic scale. The values of C_c for all treated samples are lower than those of natural intact sample at consolidation pressure of up to 70 kPa because the compressibility of reconstituted samples is less in the vicinity of yield stress (Fig. 6b). The compression indices of reconstituted samples increase rapidly after yield point. When the consolidation pressure reaches between 1 to 2 times of yield stress, samples behave inversely at different cement contents. Udaka et al. [25] also discussed the similar behavior of cement-treated Japanese marine clays. Compression indices of natural intact, 1% and 2% cemented samples become almost constant when the pressure exceeds 1.7 times of yield stress. However, for 3%, 4%, and 6% cement content samples, the compression indices sustain their increasing behavior with consolidation pressure even beyond the vicinity of yield stress.

The compression behavior of natural and reconstituted samples at 7 days curing and 50 kPa reconstituted pressure is established in Fig. 7. The initial void ratio (e_0) and swell index (C_s) of the natural intact sample is the closer to the 1% cemented sample. However, the post-yield curve of the intact sample is parallel to the post-yield curve of 2% cemented sample. And the values of pre-consolidation pressure and compression index of the natural intact sample are close to the values of yield stress, and compression index of 2% cemented sample. The compression characteristics (C_c and σ_y) of 3% cemented sample are higher, and compression characteristics of the untreated sample are lower than those of the natural intact sample. The C_c-curves of natural and reconstituted samples are shown in Fig. 7b. For the naturally structured marine clays, compression index becomes maximum when the consolidation pressure exceeds pre-consolidation pressure, afterwards it gradually decreases and tends to become constant [25]. The C_c-curve of 1% cemented sample shows similar behavior. However, the C_c-curve behavior of 2% cemented sample is more identical to the natural intact one.

4.2.2 Effect of reconstituted pressure

Figure 8 shows a comparison of the natural sample with 2% cemented samples reconstituted under 50 and 98 kPa. Sample reconstituted under 98 kPa has higher values of yield stress, and low values of compression and swell indies as compared to sample reconstitutes at 50 kPa and the natural intact sample as shown in Fig. 8a. Zhang et al. [32] determined that the increment in the consolidation pressure during the reconstitution of clays induces more strength and decreases the compressibility. Moreover, the behavior of C_c-curve of 98 kPa reconstituted sample is not similar to C_c-curve of intact sample in the pre-yield region and also has lower C_c-value than intact sample in the post-yield region (Fig. 8b). On the other hand, sample reconstituted under 50 kPa have the same values of σ_y and C_c, and its C_c-curve trend is also identical to the intact sample in pre- and post-yield region.

4.2.3 Effect of curing time on the reconstituted method with respect to compression characteristics

Effect of curing time on compression characteristics of 2% cemented samples is illustrated in Fig. 9. The 7 days' cured samples have higher initial void ratio and swell index as compared to 14- and 28-days' cemented samples as shown in Fig. 9a. It indicates that inter-aggregate pores have large size at an initial stage and are filled by cementitious material due to pozzolanic reaction with increasing curing time [40]. The effect of curing time on the σ_y- and C_c-values of 2% cemented samples is insignificant. These values are almost equal to σ_p and C_c of the intact sample. The C_c-curves of 2% cemented samples at different curing times shows a similar trend to the natural intact one (Fig. 9b).

4.3 Consolidated undrained triaxial test

Previous studies have revealed that the effect of structure on the mechanical behavior of Shanghai clay can be observed in the undrained triaxial tests [5,9,59]. Therefore, consolidated undrained triaxial (CU) tests were performed on natural and artificially structured clays, and artificially structured clays were reconstituted under 50 kPa from oedometer test findings. The curing times of reconstituted samples were 7, 14 and 21 days. Usually, reconstituted samples display strain hardening behavior at the effective confining pressure of lower than the yield stress [27,60,61]. To avoid the influence of over-consolidation, effective confining pressures for all tested samples were more than their yield stress. The natural intact sample was tested with three different effective confining pressures (100, 200, and 300 kPa) while for artificially structured samples, effective confining pressure was 200 kPa.

4.3.1 Stress-strain and excess pore pressure behavior

The behaviors of deviatoric stress (q), excess pore pressure (u), and stress ratio are discussed in Fig. 10. It is seen that cement content has a significant influence on q and u, and the peak q- and u-values increases with increasing the cement content [63]. However, the increment in u is not meaningful. The q and u generate rapidly at the lower strain level in tested samples. The increasing behavior of q continues even after 20% of strain, however, the generation of the u

decreases after attaining a peak at a specific strain range. A clear dilation can be observed in *u*-curves, and strain hardening behavior is observed in all the samples (reconstituted and natural) with positive excess pore pressure. Such strain hardening behavior is due to a large amount of silt content, and this trend is also discussed by Wang et al. [62] for low plastic fine-grained soils. The peak deviatoric stress of natural intact sample is in between 2% and 3% cemented samples. However, at 2% cement content, peak excess pore pressure and stress ratio values are almost the same as the intact one.

4.3.2 Stress paths and critical state lines

Stress paths and critical state lines of the natural intact samples are presented in Fig. 11. Initially, all stress paths move almost parallel to the q-axis due to the increase in deviatoric stress (q) in p'-q stress plane. After this, the stress paths display contractive behavior with the increment of q and the decrement of mean normal effective stress (p'). During this stage, positive excess pore water pressure is generated, and breaking of cementation bonds is also accrued. After attaining the critical state, the stress paths show dilation (strain hardening) with an increase in q as well as p'. This strain hardening behavior usually shows dense sands or over-consolidated clays during shearing. However, the tested specimens are in the normal consolidation state because the applied effective confining pressure is more than their pre-consolidation stress/yield stress [64]. This behavior of stress paths is possibly due to the large quantity of silt content [62]. The critical state lines (CSL) of the natural intact sample is well defined with the M-value of 1.38.

The stress paths of reconstituted samples are also shown strain hardening behavior as presented in Fig. 12. Figure 12a presents the stress paths of 1% cemented samples at 7, 14- and 21-days curing time. All samples failed on the same critical state line. Though the study shows that the M-values of highly cemented clays increases with curing time [27]; however, no clear effect of curing time on the *M*-values is found at low cement content. Similar stress paths behaviors can be seen in Fig.12b and Fig. 12c for 2% and 3% cemented samples respectively. The *M*-values of 1%, 2% and 3% cemented samples are 1.25, 1.4 and 1.5 respectively.

Fig. 13 illustrates the comparison of stress paths. The CSL of the natural sample is drawn with *M*-value of 1.38 in Fig. 13. The stress path of 1% cemented sample failed below, and that of 3% failed above the CSL of the natural intact sample. However, the 2% cemented sample failed on CSL of the natural intact sample and having approximately equivalent the *M*-values.

5. Microstructure results and discussion

5.1 Pore size distribution analysis

According to Lapierre et al. [38], mercury intrusion porosimetry (MIP) measures entrance pore diameter. It cannot measure the inside diameter of the pores; henceforth, it is assumed that the pore shape of soil is cylindrical.

5.1.1 Effect of cement content on the pore size distribution

Figure 14 shows a comparison of pore size distribution (PSD) of natural and reconstituted samples at 21 days curing time. On the vertical axis in Fig. 14a, $\delta V_p/\delta logD_p$ is plotted, where D_p is the pore size diameter and V_p indicates the pores volume whose diameter is D_p. The term “$\delta V_p/\delta logD_p$ “is known as pore density [65]. The pores sizes vary from 0.01μm to 300 μm in Fig. 14. The PSD curves show extra narrow peaks about 7 μm which probably could be due to two causes. Firstly, the potential samples cracking happened during the freeze-drying process, possibly of which lies in high initial water content after reconstitution. Secondly, these narrow peaks could be due to the high silt content in samples. With the addition of cement content, the pores densities of these narrow peaks reduce. It is due to cementation material that filled the large-sized pores. The PSD curves of untreated, 1% and 2% cemented samples have more pore densities at 7 μm compared to natural intact, and 3% cemented samples as shown in Fig. 14a. The densities of narrow peaks reduce with the increment of cement.

The broader peaks of natural intact, untreated, 1% and 2% cemented samples are around 0.2 μm, and the 3% cemented sample has about 0.6 μm. These curves have more pores volume as compared to narrow peaks. The pore densities of broader peaks increase with the increment of cement content due to flocculation of particles which causes to produce the pores. The cementation material fills the large pores, binds the aggregates together, converts the large pores into small pores and also increases total pore volume due to more reticulation of particles. Fig. 14b shows a relationship between cumulative pore volume and pore diameter. With an increment of cement content from untreated to 3%, total pore volume increases due to additional reticulation of particles, and it also enhances the inter-cluster bonding.

5.1.2 Effect of curing time on the pore size distribution

Figure 15 illustrates a comparison of PSD curves of natural intact sample with 2% cemented samples at different curing time. With an increment of curing time, pore densities decrease due to the formation of cementitious material as shown in Fig.15a. Figure 15b shows that pores volume larger than 1μm decreases with the curing time because cementitious material fills the large sized pores and convert them into small sized pores. However, total pores volume decreases with curing time for cemented samples. For the natural intact sample, pore volume (D_p<10 μm) is 0.14 cm^3/g and pore volume (D_p<10 μm) of 2% cemented samples varies from 0.125 to 0.155 cm^3/g with curing time. Therefore, the pores volume (D_p<10 μm) of 2% cemented samples is almost the same as natural intact one. The majority of pores are smaller than 10 μm in both 2% cemented and intact samples soil structures, and these pores dominate the mechanical behavior of both soils because the pores diameters larger than10 μm are air pores [53]. Hence, the mechanical behavior of 2% cemented samples is similar to intact one. At 21 days curing, the 2% cemented sample has the same total pore volume as the natural intact one.

5.2 Scanning electron microscope analysis

Figure 16 illustrates a comparison of typical SEM microimages of natural intact sample with the samples reconstituted at 50 kPa. The SEM image of the natural intact sample shows an open type of microstructure in Fig. 16a, with flat clay particles assembled in a dispersed arrangement and also covered large silt particles. The large sized silt particles can be identified in Fig. 16. The microstructure of Shanghai marine clay has different sizes of pores due to silt particles. It is also verified by the pore size distribution (PSD) curves as discussed in the below section. Untreated and 1% cemented samples also have an open type dispersed structure identical to the microstructure of natural intact sample as shown in Fig.16b and Fig.16c respectively. The effect of cement content cannot be observed in the case of 1% cemented sample. The microstructure of 2% cemented samples is also similar to intact one, but it exhibits some signs of particles reticulation on the left side as depicted due to the formation of calcium silicate hydrates (CSH) in Fig. 14d [66]. Figure 16e shows an SEM image of 3% cemented sample and effects of cement can be observed on microstructure in the form off reticulation and needle-shaped products. The presence of hydrated products became more evident in 3% cemented sample which produced different mechanical behavior as compared to the natural intact sample.

6. Steps and validation of reconstitution method

To reconstruct the artificially-structured marine clay identical to its natural intact clay, following are the steps of the reconstituted method:

a) Determine the physical and mechanical characteristics of the natural sample.

b) Determine the c_0-value of cement content regarding liquid limit (w_L) using Fig. 4 or Eq. 2.

c) Select immediate preceding and following percentages of the c_0-value obtained in step (b) for trial and reconstitute the samples as per described method under pre-consolidation pressure.

d) Determine the compressibility characteristics and the compression index behavior with effective consolidation pressure for reconstituted samples at different curing time.

e) Compare compressibility behavior of reconstituted samples with the intact sample and determine the most suitable percentage of cement content.

f) Compare stress-strain and stress path behaviors critical state of reconstituted and the natural intact samples.

To follow the above-described steps, the method was applied to another Shanghai marine clay with different physical characteristics as compared to the previous one. The c_0-value determined from Fig. 4 regarding w_L is 2%. Reconstituted samples were prepared at 2% and 3% cement content for trials. Compression curves of reconstituted and natural intact samples are compared in Fig. 17. Pre-consolidation pressure and compression index of the intact sample are about the same as yield stress, and compression index of 2% cemented sample. The initial void ratio, yield stress and compression index of 3% cemented sample are quite higher than those of intact one. The post-yield behavior of C_c curves of natural intact and 2% cemented samples is the same. The stress-strain behavior and the stress paths are also compared in Fig. 18. The peak deviatoric stress of intact sample is less compared to 2% and 3% cemented sample while the *M*-value, pore pressure, and stress ratio are approximately the same as 2% cemented one. The mechanical behavior of 3% cemented sample is totally different from the natural intact one. Overall, the mechanical behavior of 2% cemented sample is analogous to natural sample.

7. Conclusions

In this study, a method has been proposed to reconstruct the structured clay from the disturbed state of natural clay, identical to natural intact clay. The developed method is a promising approach for fast reconstitution of structured marine clays for quantitative element and physical model testing. The macro and micro characteristics of natural intact and artificial structured samples were compared by unconfined compression tests, oedometer tests, undrained triaxial tests, SEM analyses, and MIP tests to examine the effectiveness of the method. After the macro and micro levels evaluation of the developed method, the following conclusions can be made:

The general mechanical behavior of 2% cemented sample is analogous to the intact Shanghai marine clay at both macro and micro levels. Additionally, the method is also validated using another structured marine clay with different index properties. The values of C_c, σ_y, u, and critical state line (M-value) of artificially structured clay treated with 2% cement are similar to the natural intact clay.

A correlation is also proposed to determine the approximate c_0-value of clays from liquid limit to avoid the lengthy procedure discussed in section 3.3. The c_0-value varies from clay to clay and depends upon the index properties and cement characteristics. However, the final percentage of cement content can be determined after trials on various cement content along the c_0-value.

Overall, the proposed method is fast, economical and simple to reconstitute the artificially structured soils for quantitative studies, and can be more accurately applied to the structured marine clays of the south-east Asia region.

Acknowledgment

The financial support of the National Nature Science Foundation of China (Grant No. 41727802) is gratefully acknowledged.

References

[1] J.K. Mitchell (1976) Fundamentals of soil behavior. New York Wiley.

[2] S. Leroueil, J. Magnan, F. Tevenas, Embankments on soft clays, Ellis Horwood, New York (1990).

[3] O. Kohan, C. Gaudin, M.J. Cassidy, B. Bienen, Spudcan extraction from deep embedment in soft clay, Appl. Ocean Res. 48 (2014) 126–136.

[4] Y. Zhao, H. Liu, To ward a quick evaluation of the performance of gravity installed anchors in clay: penetration and keying, Appl. Ocean Res. 69 (2017) 148–159.

[5] S. Zhang, G.L. Ye, C. Liao, J. Wang, Elasto-plastic model of structured marine clay under general loading conditions, Appl. Ocean Res. 76 (2018) 211-220.

[6] S. Zhang, G.L. Ye, C. Liao, J. Wang, Elasto-plastic model for overconsolidated clays with focus on volume change under general loading conditions. Int. J. Geomech. 18 (3) (2018) 04018005.

[7] S. K. Yadav, G.L. Ye, Y.L. Xiong, U. Khalid, Unified numerical study of shallow foundation on structured soft clay under unconsolidated and consolidated-undrained loadings. Mar. Georesour. Geotec (2019). doi:10.1080/1064119X.2019.1576244

[8] Y.X. Wu, H.M. Lyu, J. Han, S.L. Shen, Case study: Dewatering-induced building settlement around a deep excavation in the soft deposit of Tianjin, China, J. Geotech. Geoenviron. Eng. ASCE (2019). doi:10.1061/(ASCE)GT.1943-5606.0002045

[9] J. Leng, G.L.Ye, B. Ye, D,-S. Jeng, Laboratory test and empirical model for shear modulus degradation of marine soft clays, Ocean. Eng. 146 (2017) 101–114.

[10] H. Jamali, A. Tolooiyan, M. Dehghani, A. Asakereh, B. Kalantari, Post-long-term cyclic behaviour of Coode Island Silt (CIS) containing different sand content, Appl. Ocean Res. 80 (2018) 11-23.

[11] S. Leroueil, P.R. Vaughan, The generaland congruent effects of structure in natural soils and weak rocks, Géotechniqu*e* 40 (3) (1990) 467-488.

[12] J.B. Burland, On the compressibility and shear strength of natural soils, Géotechnique 40 (3) (1990) 329-378.

[13] Z,-Y Yin, Y.F. Jin, S.L. Shen, H.W. Huang, An efficient optimization method for identifying parameters of

soft structured clay by an enhanced genetic algorithm and elastic-viscoplastic model, Acta Geotechnica12 (4) (2016) 849–867.

[14] Q.Y. Zhu, Z.-Y. Yin, P.Y. Hicher, S.L. Shen, Nonlinearity of one-dimensional creep characteristics of soft clays. Acta Geotechnica 11 (4) (2015) 887-900.

[15] Z.-Y. Yin, J.H. Yin, H.W. Huang, Rate-dependent and long-term yield stress and strength of soft Wenzhou marine clay: experiments and modeling, Mar. Georesour. Geotec. 33 (1) (2015) 79-91.

[16] Z.-Y. Yin, M. Karstunen, C.S. Chang, M. Koskinen, M. Lojander, Modeling time-dependent behavior of soft sensitive clay, J. Geotech. Geoenviron. Eng. ASCE 137 (11) (2011)1103-1113.

[17] Z.-Y. Yin, M. Hattab, P.Y. Hicher, Multiscale modeling of a sensitive marine clay, Int. J. Numer. Anal. Methods Geomech. 35 (15) (2011) 1682-1702.

[18] M.D. Liu, J.P. Carter, Virgin compression of structured soils, Géotechnique 49 (1) (1999) 43-57.

[19] M.D. Liu, J.P. Carter, Modelling the destructuring of soils during virgin compression, Géotechnique **50** (4) (2000) 479-483.

[20] L. Bjerrum, I. Rosenqvist, Some experiments with artificially sediment clays, Géotechnique 6 (1956) 124-136.

[21] R. Pusch, M. Arnold, The sensitivity of artificially sedimented organic free illitic clay, Eng. Geol. 3 (1969) 135-148.

[22] M. Kamon, T. Nagao, Engineering properties of artificially cemented clay soils, Proc. 21st Annual Meeting of JSSMFE. Sapporo (1986) 389-390.

[23] T. Tsuchida, M. Kobayashi, J. Mizukami, Effect of aging of marine clays and its duplication by high temperature consolidation, Soils Found. 31 (4) (1991) 133-147.

[24] G. Meijer, J. Dijkstra, A novel methodology to regain sensitivity of quick clay in a geotechnical centrifuge, Can. Geotech. J. 50 (90) (2013) 995-1000.

[25] K. Udaka, T. Tsuchida, Y. Imai, Y.X. Tang, Compressive characteristics of reconstituted marine clays with developed structures by adding a small amount of cement, Japanese Geotech. J. 8 (3) (2013) 425-439. DOI: 10.3208/jgs.8.425

[26] J.K. Mitchell, K. Soga, Fundamentals of Soil Behavior, 3rd ed. John Wiley & Sons, Hoboken, New Jersey, 2005.

[27] A.H.M. Kamruzzaman, S.H. Chew, F.H. Lee, Structuration and destructuration behavior of cement-treated Singapore marine clay, J. Geotech. Geoenviron. Eng.135 (4) (2009) 573-589.

[28] S. Horpibulsuk, R. Rachan, Y. Raksachon, Role of fly ash on strength and microstructure development in blended cement stabilized silty clay, Soils Found. 49 (1) (2009) 85-98.

[29] S. Horpibulsuk, R. Rachan, A. Chinkulkijiniwat, Y. Raksachon, Analysis of strength development in cement-stabilized silty clay from microstructural considerations, Const. Build. Mater. 24 (10) (2010) 2011-2021.

[30] M.M. Rahman, A. Siddique, M.K. Uddin, Microstructure and chemical properties of cement treated soft Bangladesh clays, Soils Found. 50 (1) (2010) 1–7.

[31] T. Eskisar, Influence of cement treatment on unconfined compressive strength and compressibility of lean clay with medium plasticity, Arab J. Sci Eng. 40 (2015) 763-772.

[32] R. J. Zhang, J. Zheng, X. Bian, Experimental investigation on effect of curing stress on the strength of cement-stabilized clay at high water content, Acta Geotechnica 12 (4) (2017) 921-936.

[33] E. Mengue, H. Mroueh. L. Lancelot, R.M. Eko, Mechanical improvement of a fine-grained lateritic soil treated with cement for use in road construction, J. Mater. Civ. Eng. 29 (11) (2017) 04017206.

[34] K. Uddin, A.S. Balasubramaniam, D.T. Bergado, Engineering behavior of cement-treated Bangkok soft clay, Geotech. Eng. 28 (1) (1997) 89-119.

[35] J.H. Yin, C.K. Lai, Strength and stiffness of Hong Kong marine deposits mixed with cement, Geotech. Eng. 29 (1) (1998) 29-44.

[36] D.W. Zhang, Z. Cao, T. Zhang, X.J. Su, Effect of carbonation on leaching behavior, engineering properties and microstructure of cement-stabilized lead-contaminated soils, Environ. Earth. Sci. 76 (2017) 724.

[37] D.W. Zhang, L.B. Fan, S. Liu, Y.F. Deng, Experimental investigation of unconfined compression strength and stiffness of cement treated salt-rich clay, Mar. Georesour. Geotec. 31 (4) (2013) 360-374.

[38] C. Lapierre, S. Leroueil, J. Locat, Mercury intrusion and permeability of Louiseville clay, Can. Geotech. J. 27 (1990) 761-773.

[39] T.S. Nagaraj, N.S. Pandian, P.S.R. Raju, Compressibility behavior of soft cemented soils, Géotechnique 48 (2) (1998) 281-287.

[40] S.H. Chew, A.H.M. Kamruzzaman, F.H. Lee, Physicochemical and engineering behavior of cement treated clays, J. Geotech. Geoenviron, Eng. 130 (7) (2004) 696-706.

[41] D.T. Bergado, L.R. Anderson, N. Miura, A.S. Balasubramaniam, Soft ground improvement in lowland and other environments, (1996) ASCE, Reston,VA.

[42] N.D. Quang, J.C. Chai, Permeability of lime- and cement-treated clayey soils, Can. Geotech. J. 52 (9) (2015)

1221-1227.

[43] C.J. Wu, G.L. Ye, L.L. Zhang, D. Bishop, J.H. Wang, Depositional environment and geotechnical properties of Shanghai clay: a comparison with Ariake and Bangkok clays, B. Eng. Geol. Environ. 74 (3) (2015) 717-732.

[44] G.L. Ye, N. Lin, X.H. Bao, L. Gu, S.K. Yadav, Effect of Quaternary transgression and regression on the engineering properties of Shanghai soft clay, Eng. Geol. 239 (2018) 321-329.

[45] Y.S. Xu, S.L. Shen, Y.J. Du, Geological and hydrogeological environment in Shanghai with geohazards to construction and maintenance of infrastructures, Eng. Geol. 109 (2009) 241-254.

[46] L. Han, G.L. Ye, J.J. Chen, X.H. Xia, J.H. Wang, Pressures on the lining of a large shield tunnel with a small overburden: a case study, Tunn. Undergr. Sp. Tech. 64 (2017) 1-9.

[47] M.G. Li, Z.J. Zhang, J.J. Chen, J.H. Wang, A.J. Xu, Zoned and staged construction of an underground complex in Shanghai soft clay, Tunn. Undergr. Sp. Tech. 67 (2017) 187-200.

[48] M.G. Li, J.J. Chen, J.H. Wang, Y.F. Zhu, Comparative study of construction methods for deep excavations above shield tunnels, Tunn. Undergr. Sp. Tech. 71 (2018) 329-339.

[49] F.Y. Zeng, Z.J. Zhang, J.H. Wang, M.G. Li, Observed performance of two adjacent and simultaneously excavated foundation pits in soft clay, J. Perform. Constr. Facil. 32 (4) (2018) 04018040.

[50] Y.X. Tang, Y. Miyazaki, T. Tsuchida, Practices of reused dredging by cement treatment, Soil. Found. 41 (5) (2001) 129-143.

[51] ASTM D7015-04, Standard Practices for Obtaining Undisturbed Block (Cubical and Cylindrical) Samples of Soils, ASTM International, West Conshohocken, PA, 2004. DOI: 10.1520/D7015-04

[52] P. Delage, D. Tessier, M. Marcel-Audiguier, Use of the Cryoscan apparatus for observation of freeze-fractured planes of a sensitive Quebec clay in scanning electron microscopy, Can. Geotech. J. 19 (1982) 111-114.

[53] E.W. Washburn, Note on a method of determining the distribution of pore sizes in a porous material, Proc. Natn. Acad. Sci. USA 7 (4) (1921) 115-116.

[54] S. Rees, Part one: GDS introduction to triaxial testing, Published on the GDS. https://www.gdsinstruments.com/__assets__/pagepdf/000037/Part%201%20Introduction%20to%20triaxial%20testing.pdf

[55] Y.J. Du, N.J. Jiang, S.Y. Liu, F. Jin, D.N. Singh, A.J. Puppala, Engineering properties and microstructural characteristics of cement-stabilized zinc-contaminated kaolin, Can. Geotech. J. 51 (3) (2014) 289–302.

[56] Y.J. Du, M.L. Wei, K.R. Reddy, Z.P. Liu, F. Jin, Effect of acid rain pH on leaching behavior of cement stabilized lead-contaminated soil, J. Hazard. Mater. 271 (2014) 131-140.

[57] A. Casagrande, The determination of the pre-consolidation load and its practical significance, proceedings of 1st international soil mechanics and foundation engineering conference, Cambridge 3 (1936) 60-64.

[58] V. Malandraki, D.G. Toll, Triaxial tests on weakly bonded soil with changes in stress path, J. Geotech. Geoenviron. Eng., 127 (3) (2001) 282-291.

[59] J. Leng, C. Liao, G.L. Ye, D.-S. Jeng, Laboratory study for soil structure effect on marine clay response subjected to cyclic loads, Ocean. Eng. 147 (2018) 45–50.

[60] S. Horpibulsuk, Mechanism controlling undrained shear characteristics of induced cemented clays, Lowland Tech. Int. 7 (2) (2005) 9-18.

[61] I. Bushra, R. Robinson, Shear strength behavior of cement treated marine clay, Int. J. Geotech. Eng. 6 (4) (2012) 455-466

[62] S. Wang, R. Luna, J. Yang, Effect of plasticity on shear behavior of low plasticity fine-grained soil, J. Mater. Civ. Eng. 29 (3) (2017) 04016228.

[63] Z. Karabash, A.F. Cabalar, Effect of tire crumb and cement addition on triaxial shear behavior of sandy soils, Geomech. Eng. 8 (1) (2015) 1-15.

[64] U. Khalid, C.C. Liao, G.L. Ye, S.K. Yadav, Sustainable improvement of soft marine clay using low cement content: A multi-scale experimental investigation, Const. Build. Mater. 166 (2018) 634–646.

[65] P. Delage, D. Marcial, Y. Cui, X. Ruiz, Ageing effects in a compacted bentonite: a microstructure approach, Géotechnique 56 (5) (2006) 291-304.

[66] Y.J. Du, B.-W. Yu, K. Liu, N.-J. Jiang, M.D. Liu, Physical, hydraulic, and mechanical properties of clayey soil stabilized by lightweight alkali-activated slag geopolymer, J. Mater. Civ. Eng. 29 (2) (2017) 04016217.

Table 1 Characteristics of Shanghai soft marine clays

Characteristics	**Sample (Method Development)**	**Sample (Validation)**
Location	Putuo District	Minhang District
Natural Moisture Content, w_n (%)	42.25	41.89
Natural Density, (g/cm^3)	1.81	1.84
pH Value	8.25	_
Liquid Limit, w_L (%)	36.6	45.5
Plastic Limit, w_p (%)	19.66	24.15
Plasticity Index, I_p (%)	16.94	21.35
Activity	0.7	0.54
Specific Gravity, G_s	2.7	2.72
Grain Size Distribution		
Clay Content (%)	24	40
Silt Content (%)	74	59
Sand Content (%)	2	1
Strength Characteristics		
Unconfined Compression Strength, q_u (kPa)	40	38.66
Angle of Internal Friction, ϕ' (Degree)	32.8	_
Cohesion, c' (kPa)	20	_
Compression Characteristics		
Compression Index, C_c	0.325	0.27
Pre-Consolidation Stress, ??$_p$ (kPa)	50	48
Void Ratio, e_0	1.17	1.48

Table 2 Physicochemical characteristics of Ordinary Portland cement

Chemical Composition	**Values (%)**	**Physical Characteristics**	**Values**
Calcium oxide (CaO)	62.2	Specific gravity	3.16
Potassium oxide (K_2O)	0.6	Specific surface area (m^2/kg)	390
		Particle size, retained on 45 μm (%)	4.3
Sodium oxide (Na_2O)	0.4	Initial setting time (min)	45
Silicon dioxide (SiO_2)	16.3	Final setting time (min)	390
Aluminum oxide (Al_2O_3)	5.1	Compression strength (MPa), 3 days	22
Ferric oxide (Fe_2O_3)	5.2	Compression strength (MPa), 28 days	42.5
Insoluble residue	0.75		
Magnesium oxide (MgO)	5		
Sulphur trioxide (SO_3)	3.5		
Loss of ignition	3		
Alkali content	0.6		

Table 3 Atterberg's limits and minimum cement content of Japanese soft clays (Udaka et al. [25]).

Clays Location	Liquid Limit, w_L (%)	Plastic Limit, w_p (%)	Plasticity Index, I_p (%)	Minimum Cement Content, c_0 (%)
Fukuyama Port Clay A	99	45	54	6
Fukuyama Port Clay B	97.6	33.8	63.8	5
Osaka Bay Clay	83.3	34.5	48.8	3
Hiroshima Harbor Clay	97.1	40.7	56.4	7.1
Tokyo Haneda Clay	113.2	49.6	63.6	7.5

Table 4 Detail of curing time and cement content used in different analyses

Analysis	Tests	Reconstituted Pressure (kPa)	Cement Content (%)	Curing Time (Days)	Remarks
Microstructure	Scanning Electron Microscopy	98	1, 2, and 3	21	Samples dried through freeze-drying technique and tested by SEM apparatus (FEI Sirion 200)
		50	untreated, 1, 2, and 3	7, 14, and 21	
	Mercury Intrusion Porosimetry	98	1, 2, and 3	21	Samples dried through freeze-drying method and tested by MIP apparatus (AutoPore IV 9500)
		50	untreated, 1, 2, and 3	7, 14, and 21	
Compressibility Characteristics	Oedometer Test	98	1, 2, 3, 4, and 6	7, 14, and 21	Loading Sequence: 12.5, 25, 50, 100, 200, 400, 800, 1600, 800, 400, 200, 100, 50 kPa
		50	untreated, 1, 2, and 3	7, 14, and 21	
Strength Characteristics	Unconfined Compression Test	98	1, 2, 3, 4, and 6	7, 14, and 21	Tested by automatic unconfined compression machine
	CIU Triaxial Compression Test	50	1, 2, and 3	7, 14, and 21	Effective Confining Pressure: 200 kPa (For cement-treated samples) and 100, 200, and 300 kPa (For 0% cement-treated samples)
pH-Value			1, 2, 3, 4, and 6	7, 14, and 21	Used HORIBA pH meter

Figures

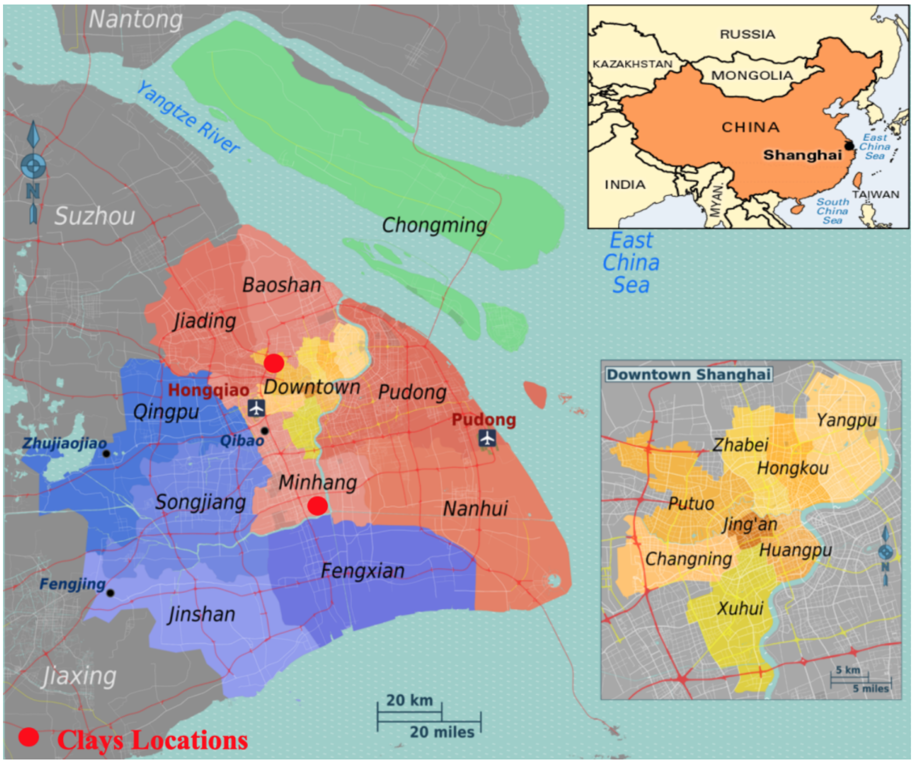

Fig. 1. Location map of Shanghai and selected clays.

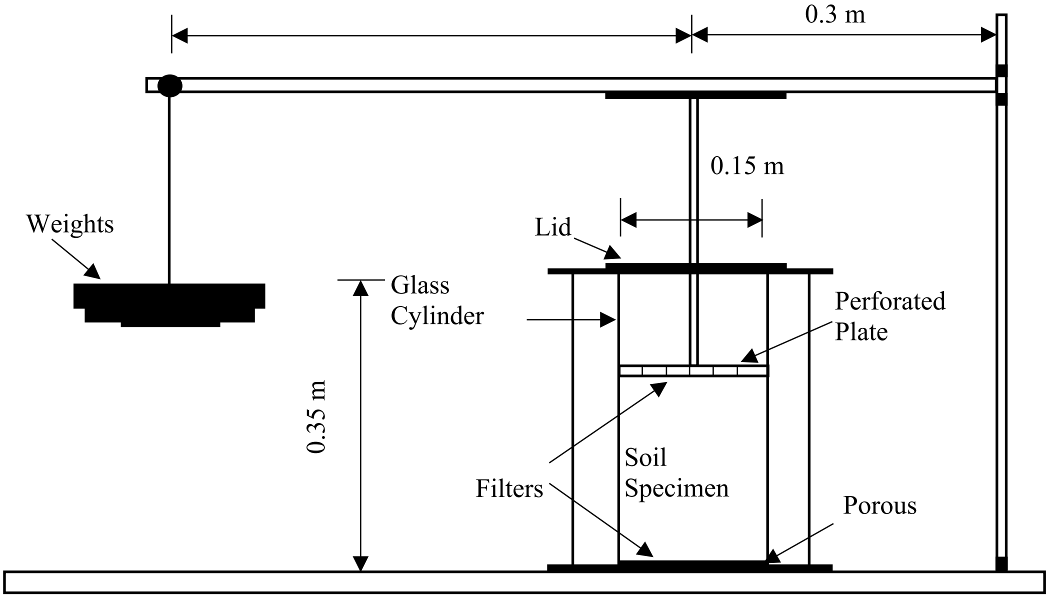

Fig. 2. Layout of consolidation tube.

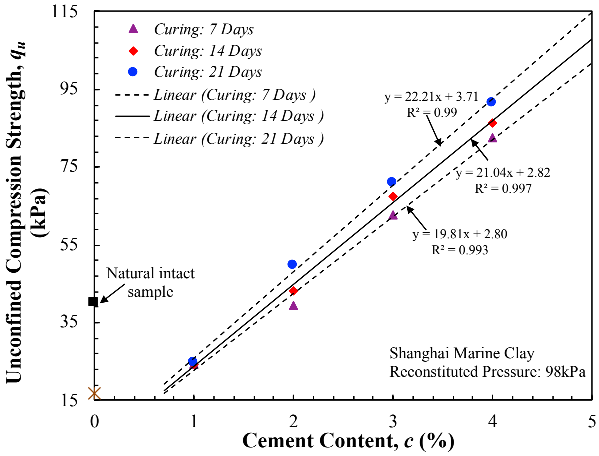

Fig. 3. Relationship between cement content and unconfined compression strength to determine minimum cement content (c_0).

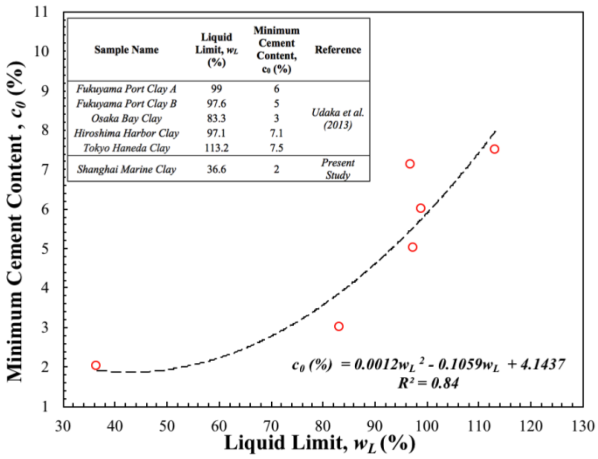

Fig. 4. Relationship between cement content and liquid limit.

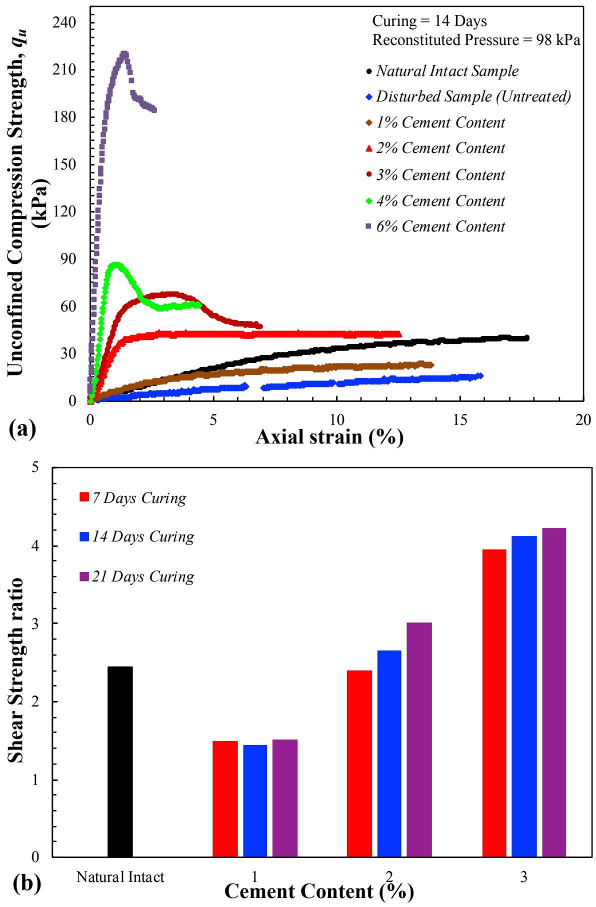

Fig. 5. Comparison of reconstituted and natural intact samples for (a) Unconfined compression strength; (b) Shear strength ratio.

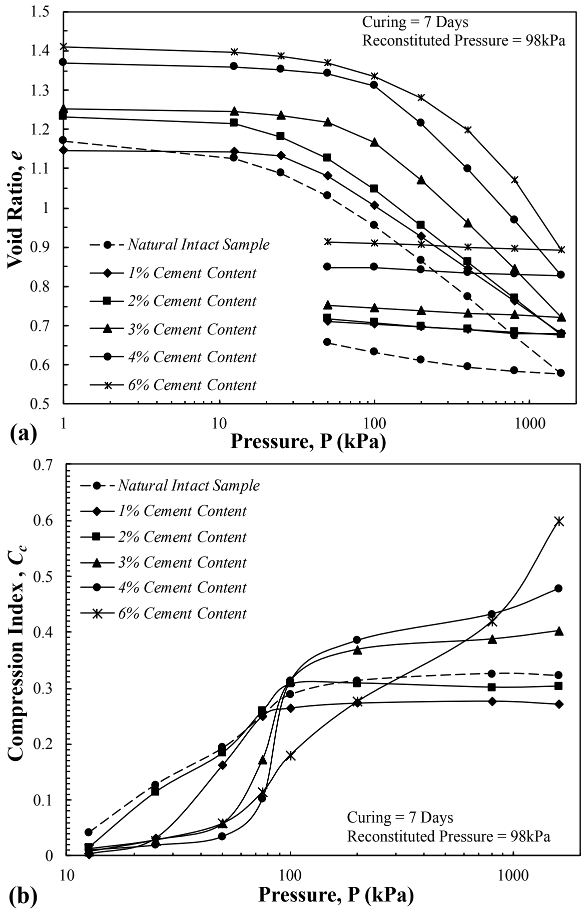

Fig. 6. Comparison between natural and reconstituted samples with different cement contents for (a) e-log(p); (b) C_c-log(p) (7 days curing and 98 kPa reconstituted pressure).

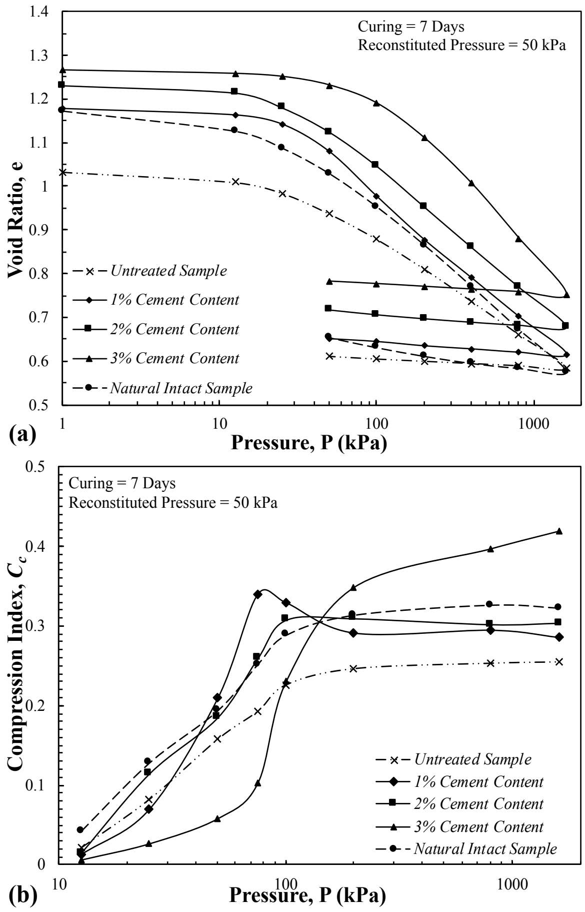

Fig. 7. Comparison between natural and reconstituted samples for (a) *e*-log(*p*); (b) C_c-log(*p*) (7 days curing and 50 kPa reconstituted pressure).

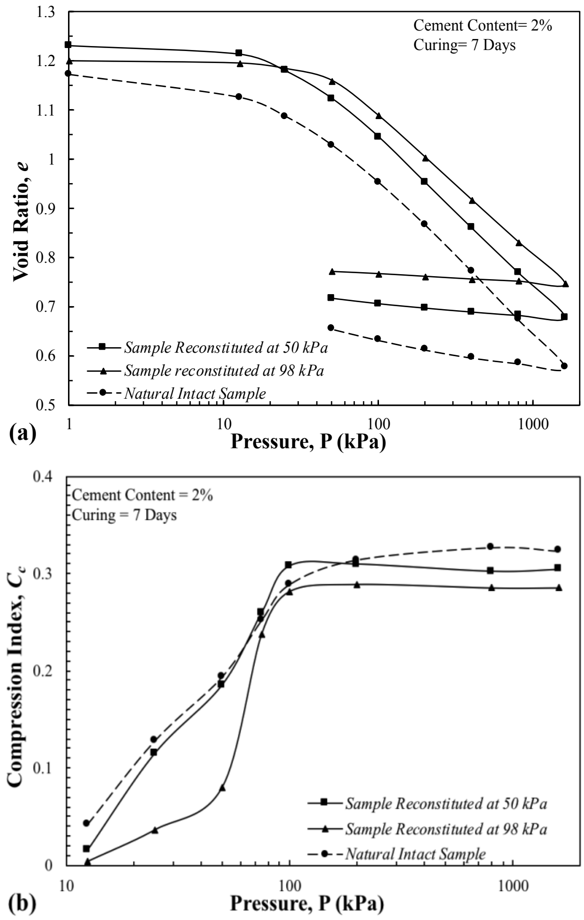

Fig. 8. Comparison between natural and reconstituted samples at different reconstituted pressures for (a) e-log(p); (b) C_c-log(p) (7days curing and 2% cement content).

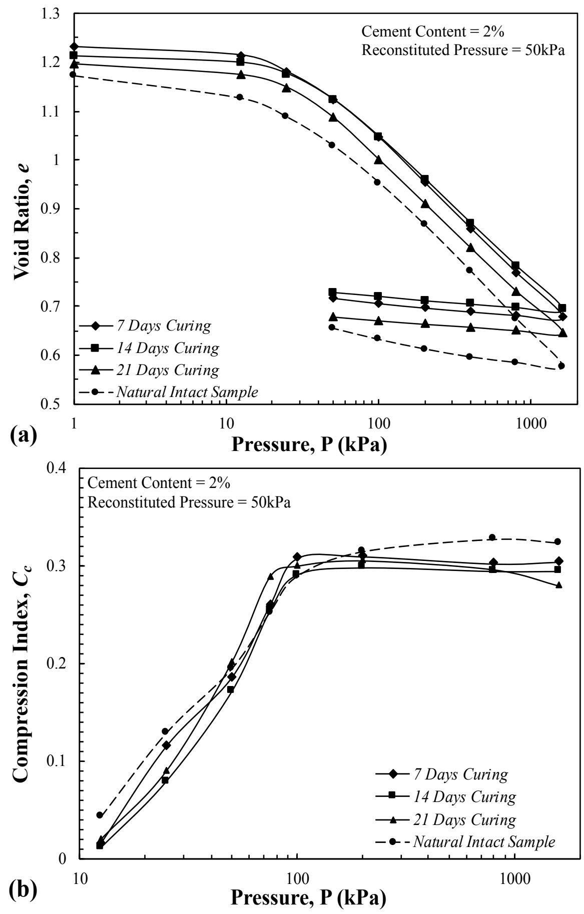

Fig. 9. Comparison between natural and reconstituted samples with different curing times for (a) e-log(p); (b) C_c-log(p) (50 kPa reconstituted pressure and 2% cement content).

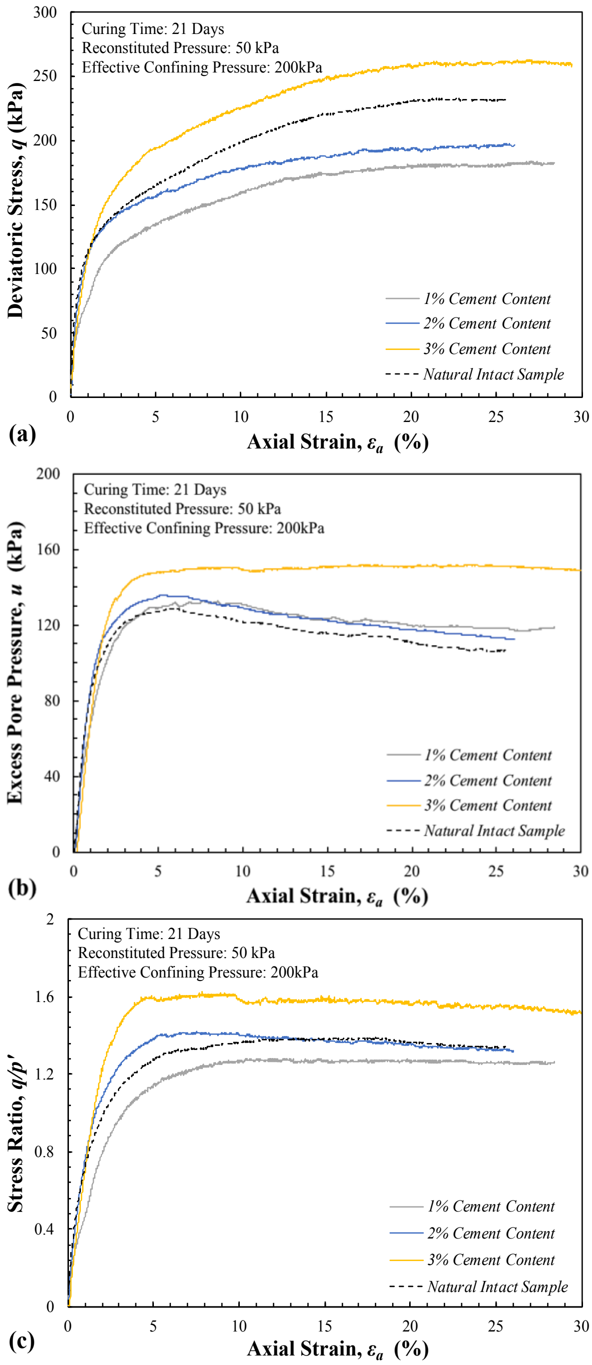

Fig. 10. Effect of cement content on (a) q-ε_a; (b) u-ε_a; (c) q/p'-ε_a.

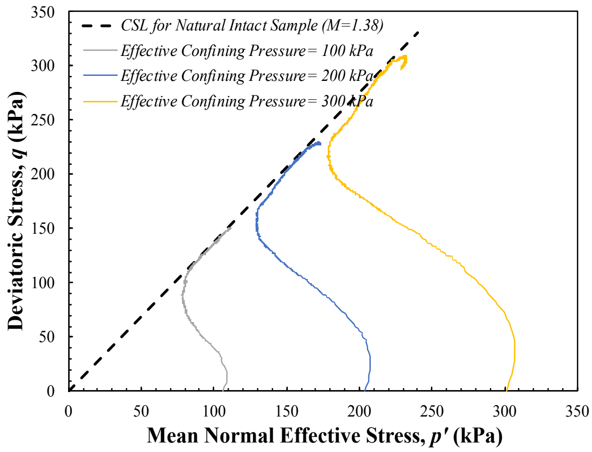

Fig. 11. Stress path and Critical state line of natural intact sample.

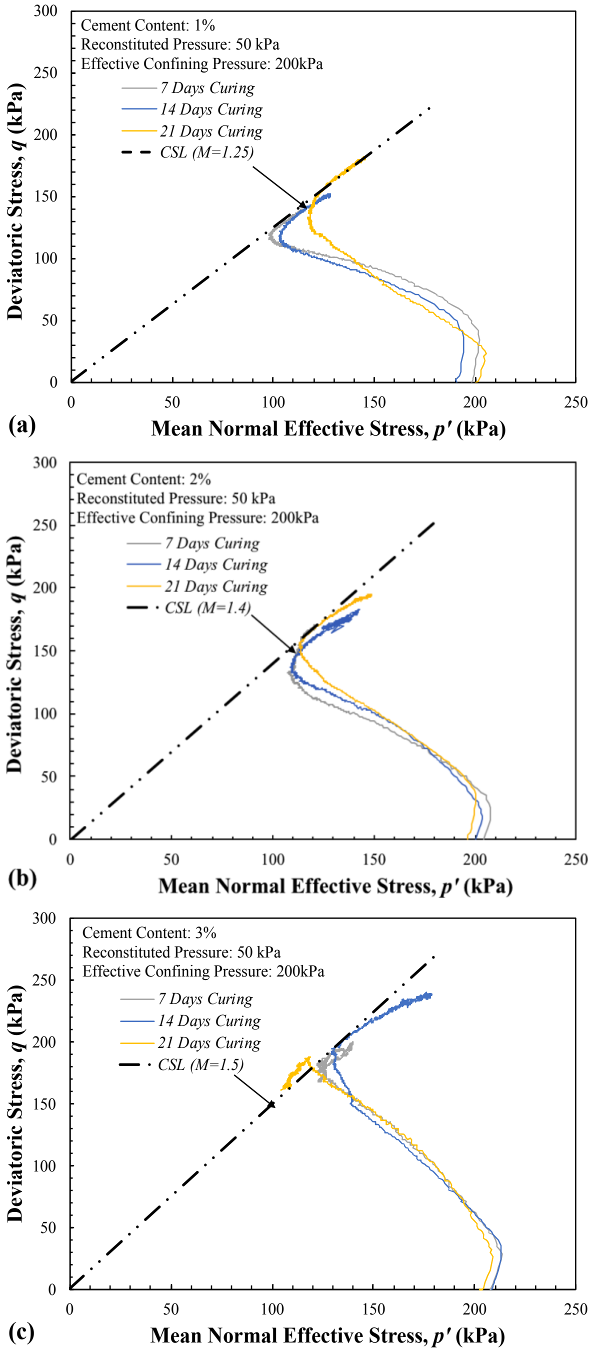

Fig. 12. Stress paths and Critical state lines of reconstituted samples at different curing times for (a) 1% cement content; (b) 2% cement content; (c) 3% cement content.

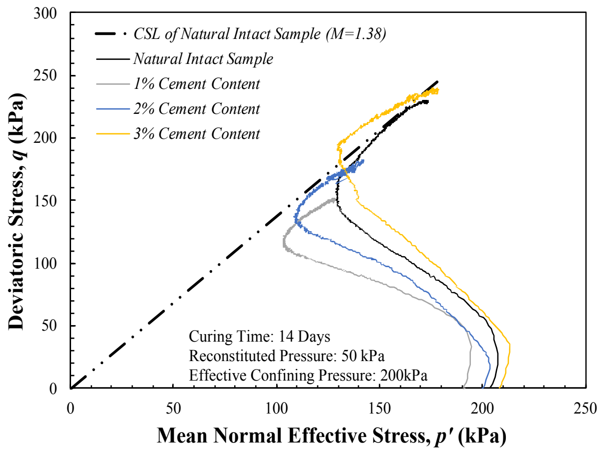

Fig. 13. Stress paths comparison between natural and reconstituted samples.

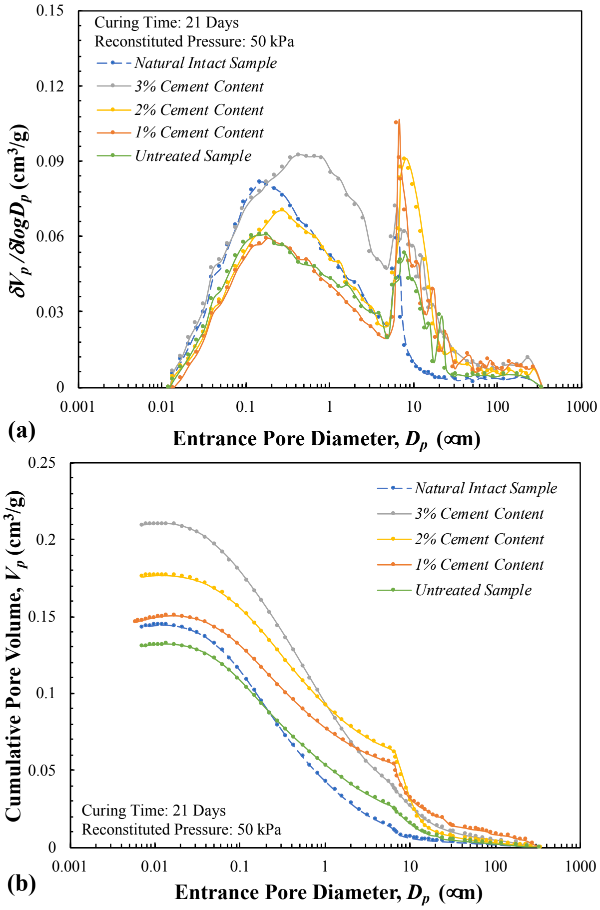

Fig. 14. Comparison of PSD curves of natural and reconstituted samples for (a) D_p-$\delta V_p/\delta logD_p$; (b) D_p-V_p.

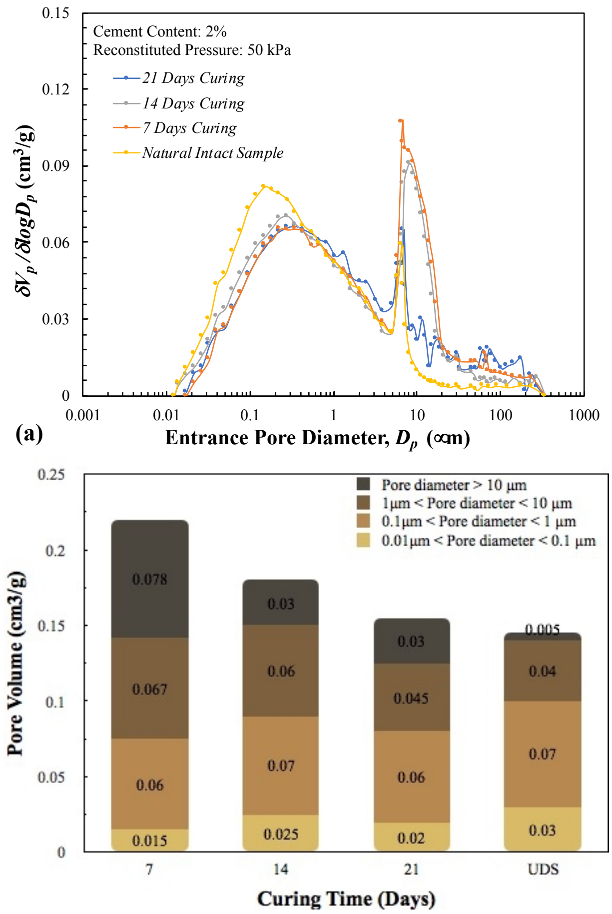

Fig. 15. Comparison of PSD curves of natural and 2% cement-treated samples at different curing times for (a) D_p-$\delta V_p/\delta logD_p$; (b) Pore volume change.

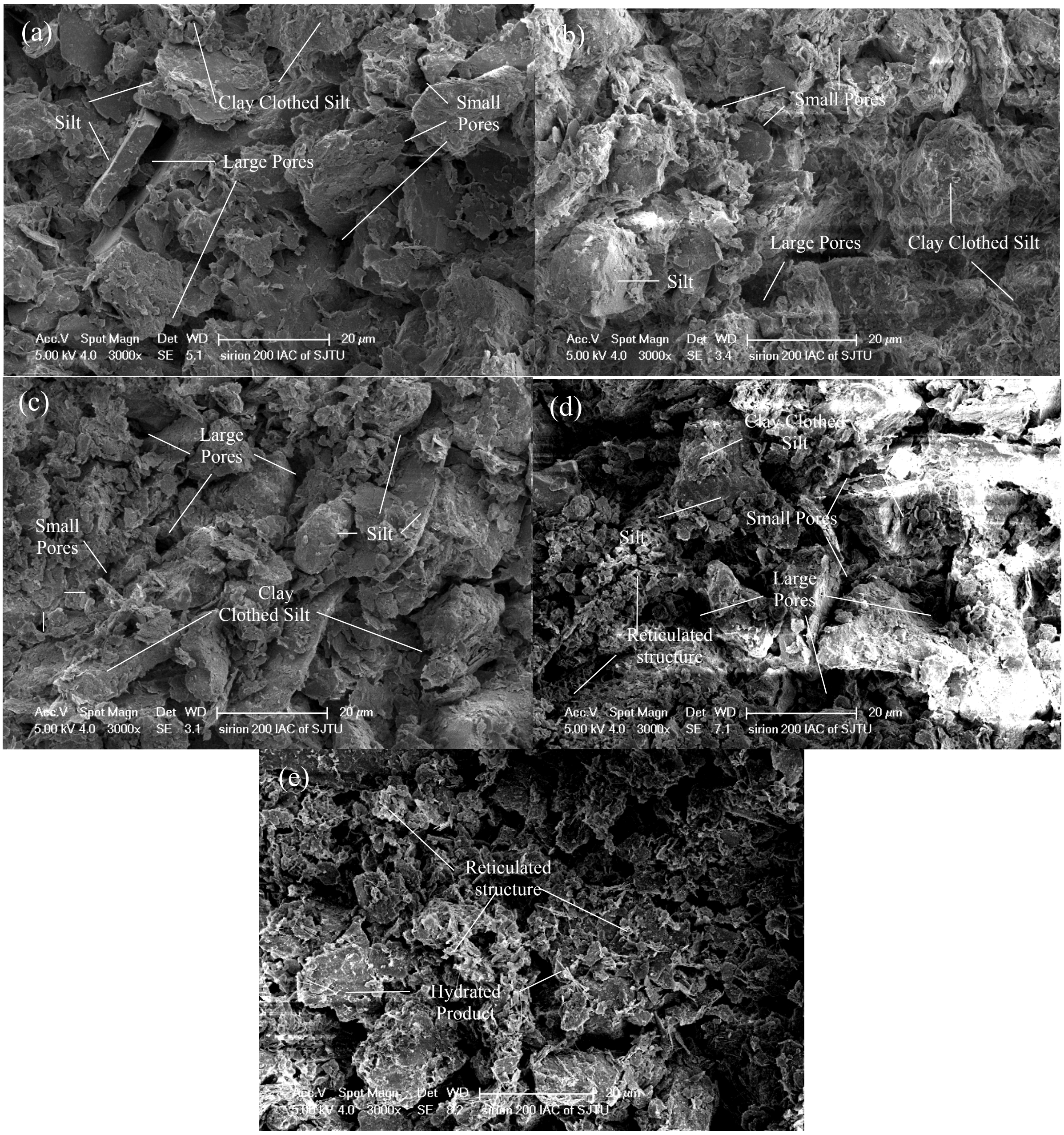

Fig. 16. Comparison of SEM images of natural and reconstituted samples at 21 days curing time for (a) Natural intact sample; (b) Untreated sample; (c) 1% cement content; (d) 2% cement content; (e) 3% cement content.

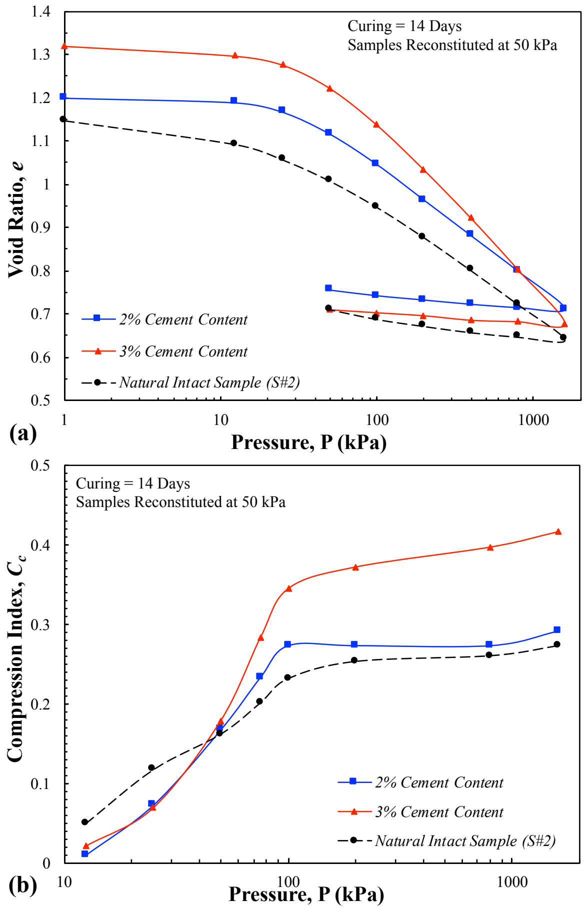

Fig. 17. Comparison between natural (S#2) and reconstituted samples for (a) *e*-log(*p*); (b) C_c-log(*p*) (14 days curing).

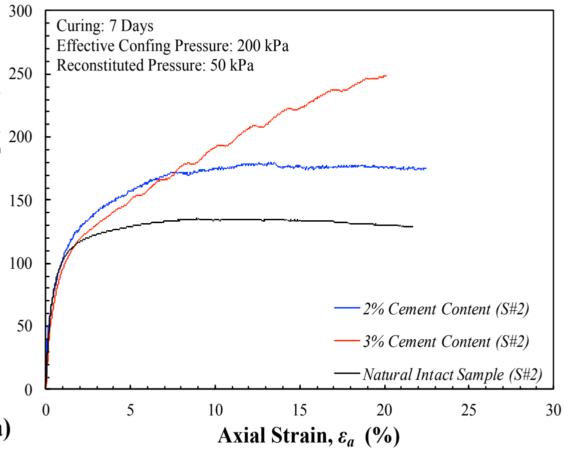
Curing: 7 Days
Effective Confing Pressure: 200 kPa
Reconstituted Pressure: 50 kPa
Deviatoric Stress, q (kPa)
2% Cement Content (S#2)
3% Cement Content (S#2)
Natural Intact Sample (S#2)
Axial Strain, εa (%)

(a)

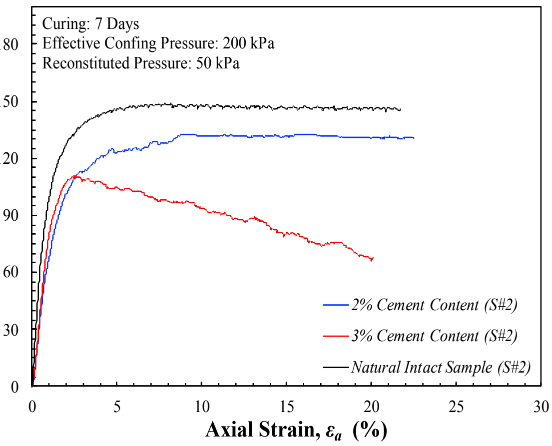
Curing: 7 Days
Effective Confing Pressure: 200 kPa
Reconstituted Pressure: 50 kPa
Excess Pore Pressure, u (kPa)
2% Cement Content (S#2)
3% Cement Content (S#2)
Natural Intact Sample (S#2)
Axial Strain, εa (%)

(b)

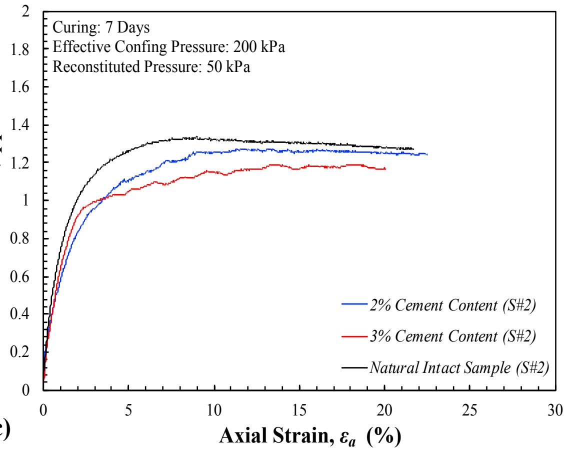
Curing: 7 Days
Effective Confing Pressure: 200 kPa
Reconstituted Pressure: 50 kPa
Stress Ratio, q/p'
2% Cement Content (S#2)
3% Cement Content (S#2)
Natural Intact Sample (S#2)
Axial Strain, εa (%)

(c)

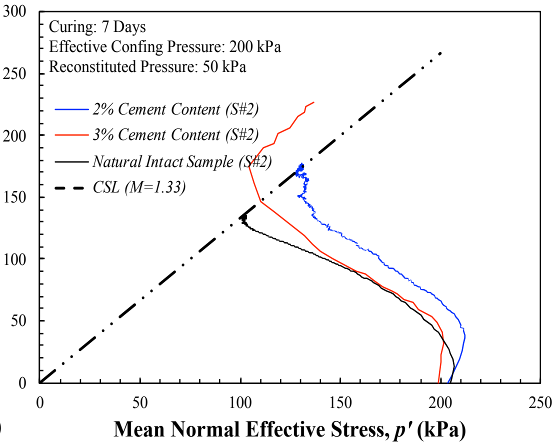
Curing: 7 Days
Effective Confing Pressure: 200 kPa
Reconstituted Pressure: 50 kPa
2% Cement Content (S#2)
3% Cement Content (S#2)
Natural Intact Sample (S#2)
CSL (M=1.33)
Deviatoric Stress, q (kPa)
Mean Normal Effective Stress, p' (kPa)

(d)

Fig. 18. Comparison between natural (S#2) and reconstituted sample for (a) q- ε_a; (b) u- ε_a; (c) q/p'- ε_a (d) q-p'